EARLY DYNAMICAL EVOLUTION OF THE MOON WITH A SUBSURFACE MAGMA OCEAN. B. G. Downey[1], F. Nimmo[1] and I. Matsuyama[2], [1]Dept. Earth and Planetary Sciences, University of California Santa Cruz, CA 95064, USA (bgdowney@ucsc.edu, fnimmo@ucsc.edu), [2]Lunar and Planetary Laboratory, University of Arizona, Tucson, AZ 85719, USA (isa@lpl.arizona.edu)

Introduction: The early thermal-orbital evolution of the Moon is important because it depended on the poorly-known initial state of the Earth [1, 2], and may have helped determine the duration of the lunar magma ocean [3] and the longevity of the Moon's magnetic field [4]. Some of this early evolution is recorded in the Moon's present-day shape and orbital characteristics.

In this work, we aim to reconstruct the thermal-orbital history of the Moon incorporating tides in the magma ocean and the effect of Cassini state transitions on its obliquity. This is in contrast to previous work, which incorporates either solid-body [3] or magma ocean tides [1] but not both. We also consider how the Moon's obliquity and eccentricity affect its shape, rather than assuming a shape that changes with the semi-major axis alone [cf. 5]. The goal is to identify the relative importance of different tidal effects and to explore what scenarios (if any) give rise to the Moon's current inclination and eccentricity. If none do, an excitation event by close encounters [6] may be required.

Thermal-Orbital Evolution: To couple the orbital and tidal effects, we use the Mignard equations from [1] and [7] originally developed in [8], [9], and [10]. These track the Moon's semi-major axis, eccentricity, and inclination among other quantities as tides in the Earth and the Moon compete to control the Moon's orbit. Generally speaking, tides in the Earth increase the Moon's semi-major axis, increase its eccentricity, and decrease its inclination. Likewise, eccentricity and obliquity tides in the Moon will decrease its eccentricity and inclination, but have little effect on its semi-major axis. Tides in the Earth are modelled as having a constant time lag, Δt, which we vary in our simulations. Tides in the Moon have two components, one in the subsurface magma ocean and one in the shell. Tides in the magma ocean are calculated from [11]'s formulation of energy dissipation in an ocean due to bottom drag. Tides in the shell are based on the heat production equations in [12] for eccentricity tides and are scaled to include obliquity tides. In all, eccentricity and obliquity tides in the Moon have both a solid-body and an ocean component, meaning that we predict higher rates of tidal dissipation than in previous studies of the Earth-Moon system.

Cassini States: We assume that the Moon is always in a damped Cassini state, and so for a given inclination, the Moon will have a specified obliquity (e.g., [1]). The Cassini state relation depends on the Moon's J_2 and C_{22} degree-2 gravity coefficients which, for a deformable body, themselves depend on the Moon's eccentricity and obliquity. There is thus a feedback between obliquity and shape, which was neglected in previous studies. During the Cassini state transition at around 30 Earth radii, the Moon's obliquity has the potential to be excited to very large values. As such, we have developed expressions for J_2 and C_{22} that depend on the Moon's eccentricity and obliquity up to fourth-order.

Magma Ocean Solidification: The magma ocean thickness is an important variable when calculating the tidal dissipation rate, and the timing of the magma ocean's complete solidification is an important way of comparing our thermal-orbital evolution study to those that use a chiefly petrologic lens (e.g., [13]). We use the rule of thumb as in [7] that 80% of a layer of magma ocean that solidifies sinks, and 20% floats and adds to the crustal thickness. Heat from tides in the ocean and shell slow the cooling process, but only in cases of extreme tidal heating is the ocean able to be remelted considerably.

Laplace Plane: The closer the Moon is to the Earth, the more skewed the Moon's Laplace plane will be towards the Earth's equator. The farther away the Moon is, the more it will be skewed towards the ecliptic. We use the equations in [14] to keep track of the inclination of the Laplace plane with respect to Earth's equator and the ecliptic. Tides will damp the Moon's orbit to the Laplace plane, so the value of the inclination that we calculate is the angle between the Moon's orbit and the instantaneous Laplace plane for a particular semi-major axis and Earth obliquity and J_2.

Results: Fig. 1 shows preliminary results of our model where the colors represent different tidal time lags of the Earth, Δt_E (see caption for more details). Fig. 1a shows how semi-major axis a evolves with time, with smaller Earth time lags resulting in slower outwards motion. Fig. 1b shows the evolution of the Moon's inclination, i, with respect to the instantaneous Laplace plane. The initial inclination is zero with respect to the Earth's equator (the Laplace plane at small semi-major axis – Fig 1h). Its subsequent evolution is controlled by both the change in the orientation of the Laplace plane and the tendency of obliquity tides to damp the inclination towards this plane. As can be seen, some scenarios succeed in reproducing the Moon's present-day inclination

(horizontal blue line). Fig. 1c shows the lunar orbit eccentricity, which increases with a due to torques from the Earth; e reaches the present-day value in most cases, because eccentricity tidal heating and damping are weak. Fig. 1d shows the obliquity of the Moon, which becomes very large as the Cassini state transition distance is approached; obliquity tides in the magma ocean, which are large, can delay the onset of the high obliquity.

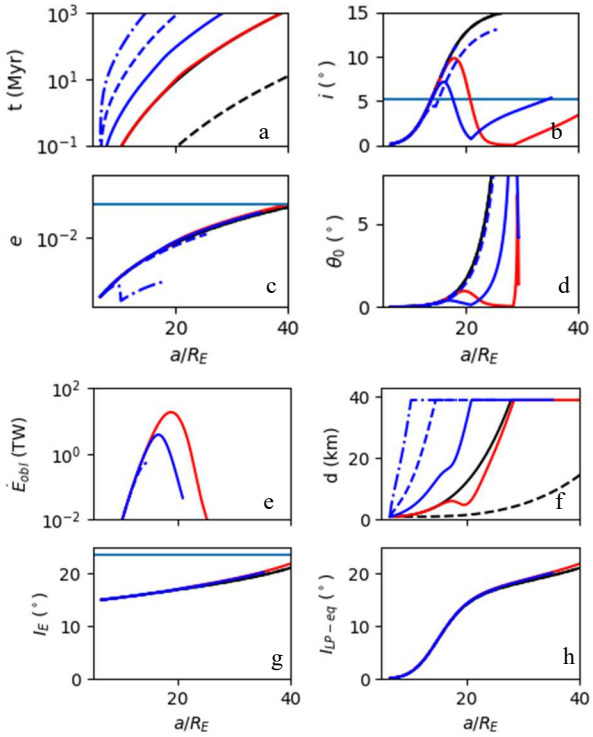

Fig. 1: The evolution of the Moon for various tidal time lag scenarios: $\Delta t_E = 10\ s$ without magma ocean heating (black), $\Delta t_E = 1000\ s$ without magma ocean heating (black-dashed), $\Delta t_E = 10\ s$ with magma ocean heating (red), $\Delta t_E = 1\ s$ with magma ocean heating (blue), $\Delta t_E = 0.1\ s$ with magma ocean heating (blue-dashed), and $\Delta t_E = 0.01\ s$ with magma ocean heating (blue dashed-dot). Horizontal blue lines denote present-day values. R_E is Earth radius. See text for more details.

Fig. 1e plots the obliquity tidal heating in the magma ocean, demonstrating that it can reach large values if the magma ocean is still in existence when the Cassini state transition is approached. Fig. 1f plots the growth of the lunar crust, which also shows the history of the magma ocean. Typical lifetimes are of order 100 Myr; but the distance at which the magma ocean solidifies is important because it determines the maximum rate of obliquity heating (Fig. 1e). Fig 1g shows how the Earth's obliquity evolves towards the present-day value, and Fig 1h shows the evolving angle between the Moon's Laplace plane and the Earth's equator.

Summary: Fig 1 shows that the present-day state of the Earth and Moon can be reached with Earth Δt_E values in the range 1-10s. This is consistent with [1] but occurs because some inclination damping is required (Fig 1b), which in turn requires outwards motion that is sufficiently rapid that the magma ocean survives out to large (~20 R_E) semi-major axes (Fig 1f). The low Δt_E value indicates low dissipation values in the Earth, perhaps due to its highly molten nature.

Future Work: The question of when and for what orbital parameters the Moon acquired its fossil bulge is still outstanding [15, 16] and will be the focus of future work. We will capitalize on our calculation of how the Moon's J_2 and C_{22} coefficients depend on eccentricity and obliquity to include a fossil shape component, potentially incorporating viscoelastic effects [17]. Since the Laplace plane transition has the potential to excite the Moon's eccentricity and inclination through resonances [2], will also more closely monitor this transition particularly for different sets of initial conditions.

References: [1] Chen, E. M., & Nimmo, F. (2016). *Icarus*, *275*, 132-142. [2] Ćuk, M., Hamilton, D. P., Lock, S. J., & Stewart, S. T. (2016). *Nature*, *539*(7629), 402-406. [3] Tian, Z., Wisdom, J., & Elkins-Tanton, L. (2017). *Icarus*, *281*, 90-102. [4] Dwyer, C. A., Stevenson, D. J., & Nimmo, F. (2011). *Nature*, *479*(7372), 212-214. [5] Siegler, M. A., Bills, B. G., & Paige, D. A. (2011). *Journal of Geophysical Research: Planets*, *116*(E3). [6] Pahlevan, K., & Morbidelli, A. (2015). *Nature*, *527*(7579), 492-494. [7] Meyer, J., Elkins-Tanton, L., & Wisdom, J. (2010). *Icarus*, *208*(1), 1-10. [8] Mignard, F. (1979). *The Moon and the planets*, *20*(3), 301-315. [9] Mignard, F. (1980). *The Moon and the planets*, *23*(2), 185-201. [10] Mignard, F. (1981). *The Moon and the Planets*, *24*(2), 189-207. [11] Hay, H. C., & Matsuyama, I. (2019). *Icarus*, *319*, 68-85. [12] Garrick-Bethell, I., Nimmo, F., & Wieczorek, M. A. (2010). *Science*, *330*(6006), 949-951. [13] Maurice, M., Tosi, N., Schwinger, S., Breuer, D., & Kleine, T. (2020). *Science advances*, *6*(28), eaba8949. [14] Dobrovolskis, A. R. (1993). *Icarus*, *105*(2), 400-407. [15] Garrick-Bethell, I., Wisdom, J., & Zuber, M. T. (2006). *Science*, *313*(5787), 652-655. [16] Keane, J. T., & Matsuyama, I. (2014). *Geophysical Research Letters*, *41*(19), 6610-6619. [17] Qin, C., Zhong, S., & Phillips, R. (2018). *Geophysical Research Letters*, *45*(3), 1286-1296.